



HAL
open science

ricin b lectin-like proteins of the microsporidian encephalitozoon cuniculi and annaliia algerae are involved in host-cell invasion

Nastasia Prybylski, Maurine Fayet, Aurore Dubuffet, Frédéric Delbac, Ayhan Kocer, Christine Gardarin, Philippe Michaud, Hicham El Alaoui, Pascal Dubessay

► To cite this version:

Nastasia Prybylski, Maurine Fayet, Aurore Dubuffet, Frédéric Delbac, Ayhan Kocer, et al.. ricin b lectin-like proteins of the microsporidian encephalitozoon cuniculi and annaliia algerae are involved in host-cell invasion. *Parasitology International*, 2022, 87, pp.102518. 10.1016/j.parint.2021.102518 . hal-03925737

HAL Id: hal-03925737

<https://hal.science/hal-03925737>

Submitted on 8 Jan 2024

HAL is a multi-disciplinary open access archive for the deposit and dissemination of scientific research documents, whether they are published or not. The documents may come from teaching and research institutions in France or abroad, or from public or private research centers.

L'archive ouverte pluridisciplinaire **HAL**, est destinée au dépôt et à la diffusion de documents scientifiques de niveau recherche, publiés ou non, émanant des établissements d'enseignement et de recherche français ou étrangers, des laboratoires publics ou privés.



Distributed under a Creative Commons Attribution - NonCommercial 4.0 International License

1 **Ricin B Lectin-Like proteins of the microsporidian *Encephalitozoon cuniculi***
2 **and *Anncalia algerae* are involved in host-cell invasion.**

3 Nastasia Prybylski ^{a, b}, Maurine Fayet ^a, Aurore Dubuffet ^a, Frédéric Delbac ^a, Ayhan
4 Kocer ^c, Christine Gardarin ^b, Philippe Michaud ^b, Hicham El Alaoui ^{a, ✉}, Pascal
5 Dubessay ^{b, ✉}

6
7 ^a Université Clermont Auvergne, CNRS, Laboratoire Microorganismes: Génomes et
8 Environnement, F-63000 Clermont-Ferrand, France. Electronic address:
9 nastasia.prybylski@uca.fr; maurine.fayet@uca.fr; aurore.dubuffet@uca.fr;
10 frederic.delbac@uca.fr; hicham.el_alaoui@uca.fr

11 ^b Université Clermont Auvergne, SIGMA Clermont, Institut Pascal, F-63000 Clermont-
12 Ferrand, France. Electronic address: christine.gardarin@uca.fr;
13 philippe.michaud@uca.fr; pascal.dubessay@uca.fr

14 ^c GReD, Laboratoire "Génétique, Reproduction and Développement," UMR Centre
15 National de la Recherche Scientifique 6293, INSERM U1103, Université Clermont
16 Auvergne, Clermont-Ferrand, France. Electronic address: ayhan.kocer@uca.fr

17
18 ✉ Corresponding authors: hicham.el_alaoui@uca.fr, pascal.dubessay@uca.fr

19
20 **Abstract**

21 Microsporidia are obligate intracellular pathogens capable of infecting a wide
22 variety of hosts ranging from invertebrates to vertebrates. The infection process
23 requires a step of prior adherence of Microsporidia to the surface of host cells. A few
24 studies demonstrated the involvement of proteins containing a ricin-B lectin (RBL)
25 domain in parasite infection. In this study *Anncalia algerae* and *Encephalitozoon*

26 *cuniculi* genomes were screened by bioinformatic analysis to identify proteins with an
27 extracellular prediction and possessing RBL-type carbohydrate-binding domains,
28 being both potentially relevant factors contributing to host cell adherence. Three
29 proteins named AaRBL-1 and AaRBL-2 from *A. algerae* and EcRBL-1 from *E.*
30 *cuniculi*, were selected and comparative analysis of sequences suggested their
31 belonging to a multigenic family, with a conserved structural RBL domain despite a
32 significant amino acid sequence divergence. The production of recombinant proteins
33 and antibodies against the three proteins allowed their subcellular localization on the
34 spore wall and/or the polar tube. Adherence inhibition assays based on pre-
35 treatments with recombinant proteins or antibodies highlighted the significant
36 decrease of the proliferation of both *E. cuniculi* and *A. algerae*, strongly suggesting
37 that these proteins are involved in the infection process.

38

39 Key words: Microsporidia, *Encephalitozoon cuniculi*, *Anncaliia algerae*, invasion,
40 Ricin-B lectin, adherence

41

42 **1. Introduction**

43 Microsporidia are obligate intracellular eukaryotic parasites including over 200
44 genera and 1400 species that have been characterized [1]. Microsporidia were
45 identified more than 150 years ago as etiologic agent of the Pebrine disease in
46 silkworms with the identification of *Nosema bombycis* [2]. Microsporidia can infect a
47 wide variety of hosts ranging from invertebrates to vertebrates and are reported to be
48 involved in protists and in all major groups of animals, including human [3,4]. Thus,
49 Microsporidia can cause significant economic losses in fish and shrimp farming,
50 sericulture and beekeeping [5–7]. Microsporidia are phylogenetically classified to

51 Fungi, either as a basal branch of the Fungi or as a sister group [8–10], and most
52 likely related to the Cryptomycota [11,12].

53 The life cycle of Microsporidia is divided into three phases including the
54 infective phase, the proliferative phase and the sporogonial phase. The spore
55 constitutes the infective stage, and the only extracellular form of the parasite, able to
56 persist in the environment for months thanks to a resistant thick two-layered wall and
57 contributing to the parasite dissemination [4,13,14]. Microsporidia infect host cells
58 through a unique and highly specialized invasion process, involving a tubular
59 structure coiled within the spore termed the polar tube. After spore discharge, the
60 extruded polar tube is used for inoculating the infective sporoplasm into the host cell
61 cytoplasm, in which the parasite proliferation takes place [15–17]. Spore discharge
62 occurs in different steps, including (i) an activation phase, (ii) the increase of the
63 intrasporal osmotic pressure, (iii) the eversion of the polar tube and (iv) the passage
64 of the sporoplasm through the polar tube. However, the exact mechanism(s) of this
65 process is not well understood [18]. The conditions triggering spore activation widely
66 differ according to species. Some factors promoting spore discharge are determined
67 such as shift in environmental pH [19,20] or the concentration of various cations or
68 anions [20,21].

69 At least three major routes seem to be involved in host cell invasion by
70 Microsporidia, (i) adherence of spores to host cell receptors prior to polar tube
71 evagination, (ii) extrusion of polar tube piercing the host cell plasma membrane or (iii)
72 phagocytosis of the spore followed by the extrusion of the polar tube [22]. Several
73 studies have demonstrated the importance of some proteins in the infection process,
74 in particular in the adherence and spore germination processes. Both Spore Wall
75 Proteins (SWP) and Polar Tube Proteins (PTP) play a major role during the first

76 interactions between Microsporidia and host cell components. A few SWPs
77 interacting with heparin-like motifs and glycosaminoglycans were identified from
78 several microsporidian species such as *Encephalitozoon* spp., *N. bombycis* and
79 *Antonospora locustae* [23–28]. The spore wall EnP1 protein containing a heparin-
80 binding domain in both *Encephalitozoon cuniculi* and *Encephalitozoon intestinalis*,
81 was identified as a major functional element of the adherence process to host cells.
82 The use of exogenous recombinant proteins EnP1 or rabbit anti-EnP1 antibodies
83 decreased the adherence of the spore to host cells and subsequent infection [27]. In
84 addition, a variety of exogenous sulfated glycans have been shown to inhibit
85 *Encephalitozoon* spore invasion into host cells, probably by blocking adherence
86 process [25,27]. A gene encoding a protein associated to the ADAM (disintegrin and
87 metalloprotease) family of type I transmembrane glycoprotein was also identified in
88 the *E. cuniculi* genome. ADAM proteins are known to be involved in a variety of
89 biological processes such as cell adherence and proteolysis. The use of exogenous
90 recombinant MsADAM protein (Microsporidia ADAM) inhibited the adherence of *E.*
91 *intestinalis* spores to host cells but also reduced host cell infection by ~20%,
92 suggesting its role in both adherence and infection processes [29].

93 Some studies were conducted to characterize receptors localized on host cell
94 surface. The NbSWP26 in *N. bombycis* was demonstrated to interact with the
95 immunoglobulin-like protein BmTLP of silkworm *Bombyx mori*, highlighting its crucial
96 role in spore invasion of silkworm cells [30]. The *Encephalitozoon hellem* Polar Tube
97 Protein PTP4 was shown to be able to bind *in vitro* to the host cell surface via the
98 host transferrin receptor 1 (TfR1) protein. Interestingly, interfering with the
99 interactions between PTP4 and TfR1 led to a decrease in the infection of host cells
100 [31]. In a few microsporidian species such as *Spraguea lophii* and *N. bombycis*,

101 proteins containing a Ricin-B Lectin (RBL) domain were identified and their
102 involvement in parasite infection has been suggested or demonstrated [32,33]. Ricin
103 is a lectin glycoprotein composed of a chain A and a chain B linked by a disulfide
104 bond [34]. The B chain is a lectin that binds to cells through interactions with
105 glycolipids and glycoproteins in particular with β -linked galactose or *N*-
106 acetylgalactosamine containing glycans localized at the cell surface [35,36]. The
107 functionality of the *NbRBL* on the adherence and infection was demonstrated by
108 incubating anti-*NbRBL* antibodies with host cells and *N. bombycis* spores. The
109 results showed a significant reduction of the spore infectivity associated to a
110 decreased adherence of spores to host cells [33].

111 Lectins are biologically active proteins isolated from humans, animals, plants and
112 microorganisms. Their ability to specifically bind different types of carbohydrates and
113 their widespread occurrence suggests their importance in various cellular processes
114 such as cell adherence, apoptosis and proliferation [37]. For example, the bacteria
115 *Bordetella pertussis*, responsible of a highly contagious respiratory infectious
116 disease, possesses a filamentous hemagglutinin that promotes strong attachment of
117 the bacteria to host cells [38–40]. The attachment of *Plasmodium falciparum*
118 merozoites to erythrocytes, leading to invasion, is mediated by a parasite adhesin
119 called EBA-175 [41,42]. Regarding viruses, the influenza virus also possesses
120 hemagglutinin involved in binding to sialic acids at the host cell surface. Endocytosis
121 is a prerequisite before the fusion of the viral envelope with host endosomal
122 membrane followed by the uptake of the virus into the cell [42–44]. All these data
123 argue for an important role of pathogen adherence prior to host cell invasion.

124 In this study, by using bioinformatic tools and preliminary experimental data,
125 we selected some proteins predicted to be extracellular and possessing

126 carbohydrate-binding domains that constitute good candidates for host cell
127 adherence in *E. cuniculi*, parasite of mammals including humans and *Anncaliia*
128 *algerae*, parasite of humans and mosquitoes. Thus, two Ricin B Lectin-Like (RBLL)
129 proteins from *A. algerae*, AaRBLL-1 and AaRBLL-2 and one from *E. cuniculi*,
130 EcRBLL-1 were selected, partly on the basis of the occurrence of a Ricin-B Lectin
131 domain in their amino acid sequences. Recombinant proteins were produced in
132 bacteria or yeast in order to obtain specific antibodies that were used to localize
133 these proteins on the microsporidian spore. Recombinant proteins and mouse
134 polyclonal antibodies were then used to evaluate the involvement of microsporidian
135 RBLL proteins in adherence and infection using adherence inhibition assays.

136

137 **2. Materials and methods**

138 **2.1 Cells, reagents and parasite culture**

139 Human Fetal Fibroblasts (MRC-5) cells (ATCC CCL-171) and Human Foreskin
140 Fibroblasts (HFF) cells (ATCC SCRC-1041) were cultured in Minimum Essential
141 Medium Eagle (MEM) (Invitrogen) supplemented with 10% inactivated Fetal Bovine
142 Serum (FBS) (Invitrogen), 2 mM glutamine (Gibco), 2.5 $\mu\text{g mL}^{-1}$ amphotericin B
143 (Dutscher), 100 $\mu\text{g mL}^{-1}$ kanamycin (Pan Biotech), 25 $\mu\text{g mL}^{-1}$ gentamicin (Gibco) at
144 37°C in a humidified 5% CO₂ atmosphere.

145 *E. cuniculi* and *A. algerae* cultures were maintained in Madin-Darby Canine Kidney
146 (MDCK) cells (ATCC CCL-34) and Rabbit kidney (RK13) cells (ATCC CCL-37)
147 respectively. Confluent monolayers of cells were infected with 5×10^5 spores of either
148 *E. cuniculi* or *A. algerae* in T75 flasks. The spores were collected from culture media,
149 purified by passing through 3 μm size filters (Millipore) for *E. cuniculi* and washed
150 with sterile water for *A. algerae* to remove host cells. Spores were then concentrated

151 at 1600 x g, and stored in phosphate buffered saline (PBS) at 4°C. Spores used in
152 these experiments were counted using a Kova-cell chamber. MDCK and RK13 cells
153 were used for parasite production as they correspond to long-term production
154 systems. However, for the following growth inhibition assays, we used MRC5 and
155 HFF cells for *E. cuniculi* and *A. algerae* respectively, as they enabled a significant
156 parasite production in few days.

157

158 **2.2 Bioinformatics analysis**

159 *E. cuniculi* and *A. algerae* local and online protein databases
160 (<https://microsporidiadb.org/micro/>) (version June 2020) were screened using cellular
161 localization prediction tools. The selection of proteins with a potential localization at
162 cell surface was based on the presence of a predicted signal peptide (SignalP
163 algorithm (<http://www.cbs.dtu.dk/services/SignalP/>)) and/or subcellular localization
164 (WoLF PSORT algorithm (<https://wolfsort.hgc.jp>) (version June 2020). Protein motif
165 prediction (carbohydrate binding domain) was carried out using ExPaSy proteomic
166 tools such as InterPro (<http://www.expasy.org/tools/>). Prediction of the structure and
167 function of the selected proteins was done using the free software Phyre2 tool
168 (<http://www.sbg.bio.ic.ac.uk/~phyre2/html/page.cgi?id=index>). 3D model were
169 obtained using Ezmol tool (<http://www.sbg.bio.ic.ac.uk/ezmol/>).

170 However, AaRBLL-1 was not selected by informatics tools as no peptide signal was
171 detected and no extracellular location was predicted. Indeed, this protein was
172 obtained from a shaving approach consisting of surface protein recovering using soft
173 SDS lysis of spore combining with mass spectrometry analysis (Prybylski *et al.*, *in*
174 preparation).

175

176 **2.3 Recombinant RBLL protein production and purification**

177 The recombinant proteins were produced in *Pichia pastoris* (strain KM71H,
178 Invitrogen) for EcRBLL-1 and in *Escherichia coli* BL21-λDE3 (PROMEGA) for
179 AaRBLL-1 and AaRBLL-2.

180 The EcRBLL-1 gene (Gene Bank Accession N°: ECU08_1730) was PCR-amplified
181 from *E. cuniculi* genomic DNA using the forward primer 5'-
182 gggaattcGAAAATTCCTCATTAACAATAAC-3' and the reverse primer 5'-
183 ggctcgagccgTTAAACAATGAGACAGTCACTA-3', containing respectively *Eco*RI and
184 *Sac*II restriction sites (underlined). After digestion, the purified PCR product was
185 inserted into the corresponding sites of pPICZα-A vector (Invitrogen) and transformed
186 into *E. coli* (DH5-α). Plasmids from positive clones were purified and sequenced. After
187 linearization with the *Sac*I enzyme, plasmids were used to transform *P. pastoris*
188 *KMH71* using EasySelect *Pichia* kit (Invitrogen), and recombinant yeasts were
189 selected on YPDS- agar plates containing zeocin antibiotic (250 μg.mL⁻¹). The culture
190 and production steps were carried out according to manufacturer recommendations
191 (Invitrogen). Briefly, recombinant yeasts were cultivated at 30°C in BMGY medium
192 (1% yeast extract; 2% peptone; 100 mM of potassium phosphate, pH 6.0; 1.34%
193 YNB (Yeast Nitrogen Base); 4x10⁻⁵% biotin; 1% glycerol) during 16h until reaching ~4
194 OD₆₀₀. BMGY medium was then removed by centrifugation, and yeast cells were re-
195 suspended in the induction medium, BMMY (identical to BMGY except that glycerol
196 was replaced with methanol 0.5%). The induction of the recombinant protein
197 expression was carried out for 72h with methanol addition every 24h. The
198 supernatant of the culture was collected by centrifugation at 4000 xg for 10 min, and
199 the volume was reduced to 20 mL on 3 kDa ultrafiltration membrane using Stirred
200 Ultrafiltration Cell (Millipore®), to concentrate the recombinant proteins. Proteins

201 were then purified by Ion Metal Chromatography Affinity (IMAC) (Protino® Ni-NTA,
202 Macherey-Nagel®), and analyzed by SDS-PAGE (12%, wt/vol.).

203 In support of GenBank sequence database related to *AaRBLL-1* (GenBank
204 Accession N°: MZ547653) and *AaRBLL-2* (GenBank Accession N°: MZ547654), the
205 genes were obtained by PCR amplification from *A. algerae* genomic DNA, using the
206 primers 5'-gggatccTTTGTAATACAGGAAAGAAGCAC-3' and 5'-
207 gggctcgagCTATTTCCGAGCAAAGAGGC-3' for *AaRBLL-1* and 5'-
208 gggggatccATGCTGATATTTTTCTTAAGTATC-3' and 5'-
209 gggctcgagTTACATTCCCATTGATTTAAAACAT-3' for *AaRBLL-2*. The *Bam*HI and
210 *Xho*I restriction sites (underlined) were added at the 5' end of both primers, allowing
211 the insertion of PCR products into the pET28a plasmid (Novagen) to generate
212 pET28a-*AaRBLL-1* and pET28a-*AaRBLL-2*. After transformation of *E. coli* DH5α
213 strain and selection on LB-agar (kanamycin 30 µg.mL⁻¹) plates, plasmid DNA of
214 positive clones were purified and sequenced, and then transformed into *E. coli* BL21-
215 λDE3 strain for the expression of recombinant proteins. The expression was induced
216 with IsopropylThioGalactoside (IPTG) 1mM for 4h from a culture in exponential
217 growth (OD₆₀₀ ~ 0.4 - 0.6). Recombinant proteins were then purified by Ion Metal
218 Chromatography Affinity (IMAC) (Protino® Ni-NTA, Macherey-Nagel®), and analyzed
219 by SDS-PAGE (12%, wt/vol.).

220

221 **2.4 Polyclonal antibody production and immunoblotting**

222 Polyclonal antibodies against each recombinant *EcRBLL-1* (*recEcRBLL-1*); *AaRBLL-*
223 *1* (*recAaRBLL-1*) and *AaRBLL-2* (*recAaRBLL-2*) protein were obtained after
224 immunization of BALB/c mice. Mice were initially immunized with 100 µg of each
225 purified protein emulsified with Freund's complete adjuvant (Sigma) in the peritoneum

226 followed by four other injections of each purified protein emulsified with Freund's
227 incomplete adjuvant (Sigma). The serum was collected one week after the last
228 injection and stored at -20°C. For immunoblotting, *E. cuniculi* and *A. algerae* proteins
229 were extracted as follows: spores in Laemmli buffer (10% Glycerol, 2% SDS, 62.5
230 mM Tris-Base pH 6.8, 0.0025% bromophenol blue, 100 mM DTT) were subjected to
231 10 cycles of freezing-thawing cycles followed by 15 min of boiling. The sample was
232 centrifuged 2 min at 14 000 *xg*. Total protein extract was collected by centrifugation
233 at 14 000 *xg* for 5 min. Proteins were then separated by SDS-PAGE 12%, transferred
234 onto polyvinylidene difluoride (PVDF) membranes (Merck), and blocked with a
235 solution of PBS-milk 5% overnight at 4°C. Membranes were incubated with either
236 anti-*EcRBL-1*, anti-*AaRBL-1* and anti-*AaRBL-2* (1:200 dilution) for 2 hours at
237 37°C. The secondary antibody, a goat anti-mouse IgG (H+L), HRP Conjugate
238 (Promega) was incubated for 1 hour at RT. Membranes were revealed by
239 chemiluminescence using the Clarity Western ECL Substrate kit (Biorad).

240

241 **2.5 Immunolocalization assays (IFA) on purified spores of *E. cuniculi* and *A.*** 242 ***algerae***

243 Purified spores were fixed in PFA 4% for 20 minutes at 4°C. Purified spores were
244 incubated with glycine 0.1M for 5 min at RT. After a quick wash with PBS, a
245 saturation step was performed with a blocking solution (PBS-bovine albumin serum
246 (BSA) 1%, (wt/vol)) for one hour at RT.

247 For purified *E. cuniculi* spores, a first immunolabeling was done by incubating the
248 samples with a 1:100 dilution of anti-*EcRBL-1* mouse polyclonal antibodies for two
249 hours at RT, then washed with 0.1% Triton X100-PBS and incubated for an
250 additional hour at RT with a 1:1000 dilution of mouse IgG (H+L) secondary antibody,

251 Alexa Fluor 555 conjugate (Invitrogen). In a second time, the samples were
252 incubated with a 1:500 dilution of anti-*E. cuniculi* rabbit serum (from a naturally
253 infected rabbit) for one hour at RT, then washed with 0.1% Triton X100-PBS and
254 incubated for an additional hour at RT with a 1:1000 dilution of rabbit IgG (H+L)
255 secondary antibody, Alexa Fluor 488 conjugate (Invitrogen).

256 For purified *A. algerae* spores, samples were incubated with antibodies against
257 AaRBLL-1 or AaRBLL-2 at 1:100 for 2 hours at RT. Samples were then washed with
258 PBS and incubated for an hour at RT with a 1:1000 dilution of mouse IgG (H+L)
259 secondary antibody, Alexa Fluor 555 conjugate.

260 A staining of the genetic material of spores was performed with DAPI (4',6-diamidino-
261 2-phenylindole) at 100 $\mu\text{g}\cdot\text{mL}^{-1}$ for 5 min at RT. Coverslips were mounted with
262 Prolong Diamond Antifade Mounting (Invitrogen) and preparations were then
263 observed with an epifluorescence microscope, magnification factor x 100 (LEICA DM
264 IRB).

265

266 **2.6 Cytotoxic assay**

267 Human Fibroblast (MRC-5 or HFF) cells were seeded in 96-well-microplates at a
268 density of 2×10^4 cells/well in MEM medium supplemented with 10% inactivated
269 FBS, 2 mM glutamine, 2.5 $\mu\text{g}\cdot\text{mL}^{-1}$ amphotericin B, 100 $\mu\text{g}\cdot\text{mL}^{-1}$ kanamycin, 25 μg
270 mL^{-1} gentamicin at 37°C in a humidified 5% CO₂ atmosphere for approximately 48 h
271 to reach confluence. The medium was then replaced by fresh culture medium
272 containing different concentrations of the recombinant proteins recEcRBLL-1 and
273 recAaRBLL-2 (25 $\mu\text{g}\cdot\text{mL}^{-1}$), or anti-EcRBLL-1, anti-AaRBLL-1 and anti-AaRBLL-2
274 mouse polyclonal antibodies (1:100) to evaluate their cytotoxicity on human cells.
275 Negative control (cells with culture medium only) and positive control (cells with 20%

276 DMSO diluted in medium) were also added to each 96-well culture plate. Each
277 condition was tested in triplicate. After incubation for 7 days at 37°C in a humidified
278 5% CO₂ atmosphere, the medium was removed and replaced by tetrazolium dye
279 MTT (3-(4,5-dimethylthiazol-2-yl)-2,5-diphenyltetrazolium bromide) (Sigma Aldrich) at
280 a 1:10 dilution in culture medium. Microplates were then incubated at 37°C for 2 h
281 under slight shaking. The dye and medium were replaced by a solution of
282 DMSO:Isopropanol (1/1, v/v) and incubated for 5 min at room temperature to dissolve
283 the protein-bound dye for OD at 550 nm using a microplate reader (Multiskan FC,
284 ThermoScientific).The cytotoxic effect of the recombinant proteins and polyclonal
285 antibodies on host cells was analyzed by comparing to the negative control
286 corresponding to 100% cell growth using a Wilcox test a non-parametric test with R
287 studio software. Differences were considered significant if the *p* value was <0.05.

288

289 **2.7 *In vitro* growth inhibition assays**

290 The potential involvement of *EcRBLL-1*, *AaRBLL-1* and *AaRBLL-2* proteins in the
291 infection process was addressed through inhibition tests, aiming to block the
292 interaction between these proteins and their interactants at host cell surface, using
293 antibodies as blocking agents or recombinant proteins as competitors.

294

295 **2.7.1 Effects of Anti-*EcRBLL-1* and rec*EcRBLL-1***

296 After validation of non-cytotoxic effect of rec*EcRBLL-1* and anti-*EcRBLL-1* antibodies,
297 the anti-microsporidian assay was performed using non-cytotoxic concentrations of
298 the rec*EcRBLL-1* (25 µg mL⁻¹) and anti-*EcRBLL-1*antibodies (1:100) on *E. cuniculi*-
299 infected MRC-5 cells. Host cells were first seeded in 48 well culture plates at a
300 density of 4 x 10⁴ cells/well in the same culture medium described above. Cells were

301 allowed to grow at 37°C in a humidified 5% CO₂ atmosphere. Triplicates wells per
302 condition were created on the plate: (i) uninfected control group, (ii) infected control
303 group, (iii) infected group exposed to the diluted *recEcRBLL-1* and (iv) infected group
304 exposed to the diluted anti-*EcRBLL-1*. The uninfected control group in each plate
305 allowed measuring the background signal in the ELISA assay. When cells reached
306 confluence, the medium was replaced by fresh culture medium containing or not
307 *recEcRBLL-1* for one hour at 37°C. Meanwhile, *E. cuniculi* spores were pretreated
308 with anti-*EcRBLL-1* antibodies and incubated at 37°C for 1 h. After the incubation
309 time, 2×10^5 spores of *E. cuniculi* were added to the pretreated cells with
310 *recEcRBLL-1* for an hour. Pretreated spores were also put in contact with host cells
311 for one hour. Culture medium was removed, cells were gently rinsed with PBS and
312 fresh culture medium was added to each well. After 7 days, the culture medium was
313 removed and cells were fixed with methanol at -20°C for 30 min. Methanol was
314 removed and after a quick wash of the cells with PBS, cells were saturated with 100
315 mM Tris-2% BSA (Sigma-Aldrich) overnight. Then cells were incubated at 37°C for 1
316 h with an anti-*E. cuniculi* rabbit serum (from naturally infected rabbit) diluted at
317 1:1000 in a dilution buffer (10 mM Tris pH = 8, 150 mM NaCl, 0.05% Tween 20, 0.2%
318 BSA Sigma-Aldrich). Cells were washed five times with washing buffer (10 mM Tris
319 pH = 8, 0.05% Tween 20) and incubated at 37°C for 1h with an anti-rabbit antibody
320 (Anti-Rabbit IgG AP Conjugate, Promega) diluted at 1:10 000 in antibody dilution
321 buffer. The cells were washed five times with washing buffer and the substrate
322 solution (0.1 mM 4-méthylumbelliferyl phosphate (MUP), 1 mM MgCl₂, 50 mM
323 Na₂CO₃ pH = 9.8; Sigma-Aldrich) was added. After incubation at 37°C for 30 min
324 under slight shaking, the reaction was stopped by the addition of 3 M NaOH and the

325 fluorescence was measured with a Fluoroskan Ascent FL, using excitation and
326 detection wavelengths of 355 nm and 460 nm, respectively.

327

328 **2.7.2 Effects of Anti-AaRBLL-1, anti-AaRBLL-2 and recAaRBLL-2**

329 HFF cells were seeded on coverslips at a density of 10^5 cells per well in 24 well
330 culture plates in the same culture medium described above.

331 Once confluence was reached, on one side cells were pretreated with recAaRBLL-2
332 ($25 \mu\text{g mL}^{-1}$) for one hour at 30°C in culture medium. After the incubation time, cells
333 were put in contact with 3×10^5 spores of *A. algerae* for one hour. Culture medium
334 was then removed, cells were gently rinsed with PBS and fresh culture medium was
335 added to each well.

336 On the other side, 3×10^5 spores were pretreated with either anti-AaRBLL-1 or anti-
337 AaRBLL-2 antibodies (1:100) for an hour at 30°C . Pretreated spores were then put in
338 contact with host cells for an hour. Culture medium was removed, cells were gently
339 rinsed with PBS and fresh culture medium was added to each well. Triplicate wells
340 were done on each plate.

341 After 7 days of incubation at 30°C in a humidified 5% CO_2 atmosphere, the culture
342 medium was removed and cells were fixed in PFA 4% at 4°C for 20 min. The
343 observation and quantification of infectious foci was done using fluorescence *in situ*
344 hybridization (FISH) method.

345 A post fixation was done in 50% ethanol for 15 min followed by ethanol 100M for 10
346 min. After two wash of 15 min in PBS, a pre-hybridization was done in a solution
347 PBS: hybridization buffer (TH) (20 mM Tris-HCl pH 7.8; 0.9 M NaCl; 1X Denhardt's
348 solution (VWR Life Science) and 0.01% SDS for 15 min at room temperature,
349 followed by a 15 min incubation in TH solution. A last incubation in TH solution was

350 done for 20 min at 45°C. TH solution was replaced by the hybridization solution
351 containing 5'-Cy3-labeled *ssuRNA A. algerae* specific-probe (Eurofins)
352 GTACTATCCAGTCCGCTC-3' (ANN01-Cy3) (50 µM ANN01-Cy3 probe and 0.5 µM
353 of warmed TH at 45°C). Plates were placed at 45°C for 3 h. After this incubation, the
354 hybridization solution was removed and **two** 30 min-washes with warmed TH solution
355 were done. TH solution was replaced with PBS. DNA was stained with DAPI for 30
356 min. Coverslips were mounted with Prolong Diamond Antifade Mounting. The
357 percentage of infected cells was assessed by counting cell nuclei and infectious foci
358 in 10 randomly chosen fields from each coverslip.

359

360 **2.7.3 Statistical analysis**

361 The effects of *recEcRBLL-1* and *recAaRBLL-2* or anti-*EcRBLL-1*; anti-*AaRBLL-1* and
362 anti-*AaRBLL-2* polyclonal antibodies on the infection of host cells by either *E. cuniculi*
363 or *A. algerae* were analyzed by comparing to the infected control corresponding to
364 100% parasite growth of each independent experiment using a Wilcox test, a non-
365 parametric test with R studio software. For each independent experiment, infected
366 control was compared to each condition in order to determine if a significant
367 difference was observed. Differences were considered significant if the *p* value was
368 <0.05 and highly significant if the *p* value was <0.001.

369

370 **3. Results**

371 **3.1 Bioinformatic characterization of *EcRBLL-1*, *AaRBLL-1* and *AaRBLL-2***

372 Our strategy **allowed** us to identify in *E. cuniculi* a hypothetical protein, composed of
373 214 amino acids with a predicted molecular weight (MW) of 23.4 kDa. The *EcRBLL-1*
374 protein displayed a significant score of extracellular prediction, associated with the

375 identification of a cleavage site between the amino acids A19 and K20 related to a
376 probable peptide signal (Fig.1A). A putative carbohydrate binding domain related to
377 RBLL (Ricin-B lectin like) was identified in the region extending from the amino acids
378 aa54 to aa133 (Fig. 1A). The glycosylation pattern of *EcRBLL-1* has been analyzed
379 and has revealed the prediction of one and six potential sites for *N*-glycosylation and
380 *O*-glycosylation respectively (Fig. 1A).

381 In the same way, two hypothetical proteins, named *AaRBLL-1*(Accession Number
382 MZ547653) and *AaRBLL-2* (Accession Number MZ547654), were identified in *A.*
383 *algerae*. *AaRBLL-1* and *AaRBLL-2* are composed of 202 and 181 amino acids
384 respectively, with a deduced molecular weight of 23.4 kDa for *AaRBLL-1* and 20.2
385 kDa for *AaRBLL-2*. No signal peptide was predicted for *AaRBLL-1* whereas *AaRBLL-*
386 *2* displayed a peptide signal using the Microsporidia DB SignalP tool (version June
387 2020). WoLF PSORT online software predicted a nuclear and extracellular
388 localization for *AaRBLL-1* and *AaRBLL-2* respectively. Despite the results obtained
389 for *AaRBLL-1*, this protein was selected according to a shaving approach, aiming
390 at identifying *A. algerae* surface proteins (Prybylski et al., in preparation). The search
391 of carbohydrate binding domain highlighted a RBLL domain for both *AaRBLL-1* and
392 *AaRBLL-2* protein, localized between aa38 and aa102 and between aa65 and aa120,
393 respectively (Fig. 1A). As for *A. algerae*, putative glycosylation sites have been
394 predicted including only three *O*-glycosylation sites for *AaRBLL-1*, and one *N*-
395 glycosylation and one *O*-glycosylation site for *AaRBLL-2*.

396 The similarity between the three RBLL proteins was analyzed by sequence alignment
397 which revealed no significant homology between the protein sequences, suggesting
398 their membership to functionally distinct proteins. Hence, the identification of a RBLL
399 would not involve large amino acids sequence conservation, but might be associated

400 to specific secondary and tertiary structure organization. This hypothesis was
401 confirmed by modeling 3D structure using Phyre2 software. The three RBLL were
402 associated to similar 3D models of agglutinin and β -glucanase, and were shown to
403 comprise in majority of β -strands and a weak percentage of α -helix that are
404 frequently found in lectins (Table 1).

405

406 **3.2 Polar tube and spore wall localization of *EcRBLL-1*, *AaRBLL-1* and *AaRBLL-*** 407 **2**

408 For immunolocalization experiments, polyclonal antibodies against *EcRBLL-1*,
409 *AaRBLL-1* and *AaRBLL-2* proteins were generated by immunization of mice with
410 recombinant proteins. The recombinant proteins were systematically performed both
411 in *E. coli* and *P. pastoris* systems, but only the expression system allowing high level
412 of expression and purification was retained. After purification by IMAC, the purified
413 proteins were analyzed in SDS-PAGE, and only single band was revealed with
414 expected sizes of about 20 kDa for recAaRBLL-2 and close to 23 kDa for both
415 rec*EcRBLL-1* and recAaRBLL-1. However, as recAaRBLL-1 was insoluble and
416 purified under denaturing conditions, the recombinant protein was only used for
417 antibody production and not as competitor for growth inhibition tests.

418 Polyclonal antibodies specificity was analyzed by Western blot ~~both~~ on spore proteins
419 extracts ~~of both species and total proteins extracted from host cells, used as negative~~
420 ~~controls~~. As shown in figure 1B, only a single protein band was detected at about 28
421 kDa with anti-*EcRBLL-1* antibodies in *E. cuniculi* spore proteins, and close to 25 kDa
422 and 20 kDa with respectively anti-*AaRBLL-1* and anti-*AaRBLL-2* antibodies for spore
423 proteins from *A. algerae*. ~~However, two extra bands were detected at about 35 kDa~~
424 ~~and 30 kDa with anti-*AaRBLL-1* antibodies that could potentially correspond to other~~

425 ~~RBL proteins. Indeed, bio-informatics analysis reveals the presence of several RBL~~
426 ~~proteins in *A. algerae* proteome close to these approximate weights (data not~~
427 ~~shown)~~. Moreover, the fact that the reactive bands sizes **did** not match the predicted
428 molecular weights 23 kDa for *EcRBLL-1* and *AaRBLL-2* may be attributed to their
429 post-translational modifications such as glycosylation that was predicted on these
430 proteins. No cross hybridization with each antibody was also observed between
431 spore proteins from *E. cuniculi* and *A. algerae*.

432 To investigate the localization of *EcRBLL-1* in *E. cuniculi* spores, anti-*EcRBLL-1*
433 antibodies were used for immunofluorescence analysis (IFA). A first immunolabeling
434 was performed with the anti-*EcRBLL-1* mouse polyclonal antibodies followed by a
435 second immunolabeling using an anti-*E. cuniculi* rabbit serum (from naturally infected
436 rabbits). Fluorescence labeling demonstrated that anti-*EcRBLL-1* polyclonal
437 antibodies reacted with the extruded polar tube of the spore (**Fig. 2**). As expected the
438 anti-*Ec* rabbit serum, labeled the whole extruded polar tube as well as the spore wall
439 of mature spores. Interestingly, the merge of anti-*Ec* rabbit serum and anti-*EcRBLL-1*
440 fluorescences highlighted a define region ~~at the tip of the polar tube~~ only labeled with
441 the anti-*EcRBLL-1* polyclonal antibodies. Furthermore, the quantification of the anti-
442 *EcRBLL-1* signal intensity, confirmed the heterogeneous intensity of labeling
443 throughout the polar tube, with a higher intensity localized at the tip of the **labeling**
444 (**Fig. 2**). Localizations of both *AaRBLL-1* and *AaRBLL-2* in *A. algerae* spores were
445 also analyzed by IFA using anti-*AaRBLL-1* and anti-*AaRBLL-2* polyclonal antibodies.
446 Both *AaRBLL-1* and *AaRBLL-2* were detected on the spore wall and the polar tube.
447 However, the labelling of the spore wall was more distinct with anti-*AaRBLL-2* than
448 with anti-*AaRBLL-1* (**Fig. 3 and 4**).

449

450 **3.3 Decrease of adherence and infection using recombinant proteins**
451 **recEcRBLL-1 and recAaRBLL-2, and anti-EcRBLL-1, anti-AaRBLL-1, anti-**
452 **AaRBLL-2 antibodies as competitors of spore adherence**

453 Cytotoxic assays were performed in order to determine the cytotoxicity on host cells
454 of the recombinant proteins recEcRBLL-1 and recAaRBLL-2 used at 25 $\mu\text{g}\cdot\text{mL}^{-1}$ and
455 of the anti-EcRBLL-1, anti-AaRBLL-1 and anti-AaRBLL-2 antibodies used at a
456 dilution of 1:100. The recombinant proteins and the antibodies showed non-cytotoxic
457 effect on MRC-5 and HFF cells corresponding to the host cells of *E. cuniculi* and *A.*
458 *algerae* respectively (Fig. S1).

459 To further analyze the role of EcRBLL-1 in cell adherence/invasion, antibody and
460 recombinant protein blocking assays were performed. The effect on *E. cuniculi*
461 infection using anti-EcRBLL-1 antibodies and the recombinant protein was measured
462 by ELISA assay. Incubations of recEcRBLL-1 (25 $\mu\text{g mL}^{-1}$) or anti-EcRBLL-1 (1:100)
463 with MRC-5 cells showed a decrease in the growth of *E. cuniculi* with inhibition
464 percentages ranging from 12.3% to 23.7% (Fig. 5, Supplementary data Fig. S2 and
465 S3). Indeed, when cells were put in contact with anti-EcRBLL-1 and were infected
466 with 2×10^5 spores, a decrease on average of 12.3% in the growth of the parasite
467 was observed. In parallel, a pretreatment of cells with recEcRBLL-1 infected at $2 \times$
468 10^5 spores led to a reduction on average of 23.7% of the parasite growth ($p < 0.001$).

469 The involvement of AaRBLL-1 and AaRBLL-2 in spore adherence and infection was
470 analyzed as described previously. The growth inhibition of *A. algerae* was quantified
471 by using fluorescence *in situ* hybridization (FISH) method. Cell nuclei and infectious
472 foci in 10 randomly chosen fields from each coverslip were counted in order to
473 assess the percentage of infected cells over total cells. A pre-treatment with anti-
474 AaRBLL-1 and anti-AaRBLL-2 polyclonal antibodies or the recombinant protein

475 recAaRBLL-2 decreased the proliferation of the parasite on average by 67.6%,
476 68.5%, and 59.3% respectively (Fig. 6). No pre-treatment with recAaRBLL-1 was
477 done as the insoluble recombinant protein was purified in denaturing conditions.

478

479 **4. Discussion**

480 The adherence of intracellular parasites to host cell is the first step of the infection
481 process. In Microsporidia, spore wall and polar tube proteins play an important role in
482 the interaction between spores and host cells [27]. Several proteins that can interact
483 with host cells have already been described in particular in *N. bombycis*,
484 *Encephalitozoon spp.*, and *A. locustae* [23–28]. In the present study, candidate
485 proteins from *E. cuniculi* and *A. algerae* were selected based on the prediction on
486 several motifs such as signal peptide and a Ricin-B-lectin like domain.

487 The results of subcellular localization and glycosylation site prediction showed that
488 EcRBLL-1 and AaRBLL-2 are potential secreted proteins and that all three proteins
489 may bind to carbohydrates. However, only AaRBLL-1 does not possess a signal
490 peptide that could be explained by the fact that the algorithms used (WoLF PSORT
491 and SignalP) have been set up on genetics models which are not completely adapted
492 to Microsporidia. In this way, the protein SWP12 from *N. bombycis* was shown to be
493 present at the spore coat by IFA even though no signal peptide was predicted
494 [45,46]. The three selected proteins possess a Ricin-B-lectin domain known to be
495 important in parasite adherence and infection in Microsporidia [32,33]. The analysis
496 of RBL proteins in microsporidian species revealed a large heterogeneity in
497 sequences but also no significant analogy between the protein sequences found
498 within a same species. However, the presence of common structures in the RBLL
499 proteins, in particular like in agglutinin and β -glucanase, could be linked to the

500 conservation of the function of carbohydrate binding as exemplified by the 3D
501 prediction model (Table 1). The comparison of *A. algerae* and *E. cuniculi* proteomes
502 revealed a greater number of RBL proteins in *A. algerae* proteome (~17 for *A.*
503 *algerae* versus 6 for *E. cuniculi*). The RBL protein encoding genes are found in other
504 microsporidian species, *N. ceranae* and *S. lophii*, respectively parasites of
505 honeybees and monkfish and are organized as clusters in genome sequences. It is
506 also the case for *E. cuniculi* as RBLL genes are found in syntenic blocks including
507 our *EcRBLL-1* gene [32]. The low size of *A. algerae* genome contigs did not allow us
508 to analyze RBLL gene synteny in this genome. Campbell et al., 2013 [32]
509 hypothesized that RBL paralogs have arisen from duplication in each species and
510 may have contributed to host adaptation. Hence, this difference in the number of
511 proteins present in *A. algerae* and *E. cuniculi* could be linked to the broad host range
512 of *A. algerae* going from mammals to insects.

513 The results of immunolocalization on *E. cuniculi* and *A. algerae* spores and polar tube
514 demonstrate a heterogeneity of labelling. The difference of localizations of the three
515 proteins (dual localization on polar tube and the spore wall for *A. algerae* and
516 restricted to polar tube for *E. cuniculi*) argues for the fact that they are probably
517 functionally different during the invasion process. The more intensive labeling of
518 *EcRBLL-1* at the tip ~~polar tube~~ has questioned about the role of this protein in the
519 attachment to the host cell membrane before the piercing of the polar tube. This
520 could correspond to the tip of the polar tube or to the sporoplasm. A specific
521 sporoplasm marker needs to be developed to answer this question. Transmission
522 electron microscopy will also be helpful to address this questioning. The *A. algerae*
523 and *E. cuniculi* RBLLs may be also different from the one identified in *N. bombycis*
524 [33] as *NbRBL* was only localized at the spore wall. Despite these differences, they

525 are all involved in the host cell infection, as a significant decrease of *E. cuniculi* and
526 *A. algerae* proliferation was observed after pre-treatments of host cells with
527 recombinant proteins or microsporidian spores with polyclonal anti-RBLL proteins.
528 These results were consistent with previous results observed for *Nb*RBL binding to
529 carbohydrates and contributing to spore adherence [33]. Indeed, RBL proteins could
530 be released during spore germination as the spore content is passing through the
531 polar tube. *Ec*RBLL-1, *Aa*RBLL-1 and *Aa*RBLL-2 could then contribute to the
532 anchoring of the polar tube, by binding to host cells carbohydrates by means of the
533 Ricin-B-Lectin domain. The distance between host cell and spores being shorter for
534 germination, the sporoplasm would be internalized by endocytic mechanism into the
535 host cell ([Supplementary data Figure S1](#)).

536 However, *Ec*RBLL-1, *Aa*RBLL-1 and *Aa*RBLL-2 did not abolish the infection
537 indicating the involvement of other components in the molecular basis of spore
538 adherence. These proteins all possess a Ricin B Lectin region and it has been shown
539 that this lectin interacts with glycolipids or glycoproteins on cell surface [35,36]. Once
540 the lectin has interacted with sugar moieties of host cells, it is presumably imported
541 into endosomes into the cytosol of host cells [34].

542 RBL **proteins** are described as glycoproteins composed of two chains, a chain A
543 involved in the inhibition of protein synthesis and a chain B (lectin) interacting with
544 glycoproteins and glycolipids at the cell surface [36,47]. Ricin-B Lectins can be
545 involved in different mechanisms such as protein activity inhibition, apoptosis
546 pathways or release of cytokine inflammatory mediators [47]. Several pathogens
547 synthesize lectins often reported to be interacting with glycoconjugates on host cells
548 promoting cell adherence, invasion and colonization of host cells [48–51].
549 *Entamoeba histolytica* trophozoites, an enteric protozoan parasite, possess a cell

550 surface lectin mediating the adherence of the parasite to host galactose and N-
551 acetyl-D-galactosamine [52,53]. The secreted Microneme (MICs) and rhoptry
552 proteins (ROPs and RONs) of the protozoan parasite, *Toxoplasma gondii* play an
553 important role in host cell recognition, attachment and penetration [54]. Two MICs
554 proteins, MIC1 and MIC4, have lectin domains capable of binding to oligosaccharides
555 with sialic acid and D-galactose in the terminal position, respectively [48,55–58].
556 However, the molecular mechanism of RBL interaction with host cells is unknown in
557 Microsporidia.

558 To conclude and in order to further understand the infection process, it would be
559 interesting to identify potential cellular receptors targeted by microsporidian RBLLs at
560 the host cell surface using technics allowing the identification of protein-protein
561 interactions such as co-immunoprecipitation or pull-down approaches. In parallel,
562 functional approaches based on RNAi could help to better understand the role of the
563 RBLL proteins in adherence and infection processes in Microsporidia. Huang in 2018
564 [59] demonstrated that *A. algerae* is one of the microsporidian species that possess
565 RNA interference (RNAi) genes and could therefore constitute an appropriate model
566 for such an approach. Few studies have investigated the efficiency of using siRNA
567 targeting specific genes in Microsporidia, mainly in *N. ceranae* and *Heterosporis*
568 *saurida*, microsporidian parasites of honeybee and lizardfish respectively [60,61].
569 Finally, our findings contribute to the deciphering of the adherence of *E. cuniculi* and
570 *A. algerae* to host cells, in which *EcRBLL-1*, *AaRBLL-1* and *AaRBLL-2* may play a
571 significant role and could pave the way to develop new therapeutic/prophylactic
572 methods to control these intracellular parasites.

573

574 **Declaration of interest**

575 The authors declare no conflict of interest

576

577 **Acknowledgments**

578 This work has been supported by a grant (MENRT) of the Ministère de
579 l'Enseignement Supérieur et de la Recherche, attributed to PhD student.

580 We thank Ivan Wawrzyniack from the LMGE of University Clermont-Auvergne
581 (France) for his contribution to the genome data analysis of microsporidian species.

582

583 **References**

584

- 585 [1] A. Cali, J.J. Becnel, P.M. Takvorian, *Microsporidia*, 2nd ed., Springer
586 International Publishing, 2017. https://doi.org/10.1007/978-3-319-32669-6_27-1.
- 587 [2] K.W. Nägeli, Über die neue krankheit der Seidenraupe und verwandte
588 organismen, *Bot. Z.* 15 (1857) 760–761.
- 589 [3] J. Vávra, J. Lukeš, *Microsporidia and ‘The Art of Living Together,’* in: D.
590 Rollinson (Ed.), *Adv. Parasitol.*, 1st editio, Elsevier Ltd, 2013: pp. 253–319.
591 <https://doi.org/10.1016/B978-0-12-407706-5.00004-6>.
- 592 [4] A. Cali, P.M. Takvorian, *Developmental Morphology and Life Cycles of the*
593 *Microsporidia*, in: L.M. Weiss, J.J. Becnel (Eds.), *Microsporidia Pathog. Oppor.*,
594 1st ed., John Wiley & Sons, Inc., 2014: pp. 71–133.
595 <https://doi.org/10.1002/9781118395264.ch2>.
- 596 [5] E.S. Didier, K.F. Snowden, J.A. Shadduck, *Biology of microsporidian species*
597 *infecting mammals*, Academic Press Limited, 1998.
598 [https://doi.org/10.1016/S0065-308X\(08\)60125-6](https://doi.org/10.1016/S0065-308X(08)60125-6).
- 599 [6] M. Wittner, L.M. Weiss, *The Microsporidia and Microsporidiosis*, American
600 Society of Microbiology Press, 1999. <https://doi.org/10.1128/9781555818227>.
- 601 [7] G.D. Stentiford, J.J. Becnel, L.M. Weiss, P.J. Keeling, E.S. Didier, B.A.P.
602 Williams, S. Bjornson, M.L. Kent, M.A. Freeman, M.J.F. Brown, E.R. Troemel,
603 K. Roesel, Y. Sokolova, K.F. Snowden, L. Solter, *Microsporidia – Emergent*
604 *Pathogens in the Global Food Chain*, *Trends Parasitol.* 32 (2016) 336–348.
605 <https://doi.org/10.1016/j.pt.2015.12.004>.
- 606 [8] L.M. Weiss, T.D. Edlind, C.R. Vossbrinck, T. Hashimoto, *Microsporidian*
607 *molecular phylogeny: the fungal connection.*, *J. Eukaryot. Microbiol.* 46 (1999)
608 17S-18S.
- 609 [9] S.C. Lee, N. Corradi, E.J. Byrnes lii, S. Torres-Martinez, F.S. Dietrich, P.J.

- 610 Keeling, J. Heitman, Microsporidia evolved from ancestral sexual fungi, *Curr.*
611 *Biol.* 18 (2008) 1675–1679. <https://doi.org/10.1016/j.cub.2008.09.030>.
- 612 [10] S. Capella-Gutiérrez, M. Marcet-Houben, T. Gabaldón, Phylogenomics
613 supports microsporidia as the earliest diverging clade of sequenced fungi, *BMC*
614 *Biol.* 10 (2012). <https://doi.org/10.1186/1741-7007-10-47>.
- 615 [11] D. Corsaro, J. Walochnik, D. Venditti, J. Steinmann, K.-D. Müller, R. Michel,
616 Microsporidia-like parasites of amoebae belong to the early fungal lineage
617 Rozellomycota, *Parasitol. Res.* 113 (2014) 1909–1918.
618 <https://doi.org/10.1007/s00436-014-3838-4>.
- 619 [12] P.J. Keeling, Phylogenetic Place of Microsporidia in the Tree of Eukaryotes, in:
620 L.M. Weiss, J.J. Becnel (Eds.), *Microsporidia Pathog. Oppor.*, 1st editio, John
621 Wiley & Sons, Inc., 2014: pp. 195–202.
622 <https://doi.org/10.1002/9781118395264.ch5>.
- 623 [13] J.P. Kramer, Longevity of microsporidian spores with special reference to
624 *Octosporea muscaedomesticae* flu, *Acta Protozool.* 8 (1970) 217–224.
- 625 [14] J. Vávra, J.I.R. Larsson, Chapter 1: Structure of Microsporidia, in: L.M. Weiss,
626 J.J. Becnel (Eds.), *Microsporidia Pathog. Oppor.*, First edit, John Wiley & Sons,
627 Inc., 2014: pp. 1–70. <https://doi.org/10.1002/9781118395264.ch1>.
- 628 [15] G.J. Leitch, G.S. Visvesvara, Q. He, Inhibition of microsporidian spore
629 germination, *Parasitol. Today.* 9 (1993) 422–424. [https://doi.org/10.1016/0169-](https://doi.org/10.1016/0169-4758(93)90052-H)
630 [4758\(93\)90052-H](https://doi.org/10.1016/0169-4758(93)90052-H).
- 631 [16] J. Schottelius, C. Schmetz, N.P. Kock, T. Schüler, I. Sobottka, B. Fleischer,
632 Presentation by scanning electron microscopy of the life cycle of microsporidia
633 of the genus *Encephalitozoon*, *Microbes Infect.* 2 (2000) 1401–1406.
634 [https://doi.org/10.1016/S1286-4579\(00\)01293-4](https://doi.org/10.1016/S1286-4579(00)01293-4).

- 635 [17] G.J. Leitch, C. Ceballos, Effects of host temperature, and gastric and duodenal
636 environments on microsporidia spore germination and infectivity of intestinal
637 epithelial cells, *Parasitol. Res. Res.* 104 (2008) 35–42.
638 <https://doi.org/10.1007/s00436-008-1156-4>.
- 639 [18] Y. Xu, L.M. Weiss, The microsporidian polar tube: A highly specialised invasion
640 organelle, *Int. J. Parasitol.* 35 (2005) 941–953.
641 <https://doi.org/10.1016/j.ijpara.2005.04.003>.
- 642 [19] A.H. Undeen, S.W. Avery, Germination of experimentally nontransmissible
643 microsporidia, *J. Invertebr. Pathol.* 43 (1984) 299–301.
644 [https://doi.org/10.1016/0022-2011\(84\)90156-3](https://doi.org/10.1016/0022-2011(84)90156-3).
- 645 [20] A.H. Undeen, N.D. Epsky, In vitro and in vivo germination of *Nosema locustae*
646 (*Microspora: Nosematidae*) spores, *J. Invertebr. Pathol.* 56 (1990) 371–379.
647 [https://doi.org/10.1016/0022-2011\(90\)90124-O](https://doi.org/10.1016/0022-2011(90)90124-O).
- 648 [21] E. Frixione, L. Ruiz, A.H. Undeen, Monovalent cations induce microsporidian
649 spore germination in vitro, *J. Euk. Microbiol.* 41 (1994) 464–468.
650 <https://doi.org/10.1111/j.1550-7408.1994.tb06043.x>.
- 651 [22] F. Delbac, V. Polonais, The microsporidian polar tube and its role in invasion,
652 *Subcell. Biochem.* 47 (2008) 208–220. https://doi.org/10.1007/978-0-387-78267-6_17.
- 653
- 654 [23] L. Chen, R. Li, Y. You, K. Zhang, L. Zhang, A Novel Spore Wall Protein from
655 *Antonospora locustae* (*Microsporidia: Nosematidae*) Contributes to Sporulation,
656 *J. Eukaryot. Microbiol.* 64 (2017) 779–791. <https://doi.org/10.1111/jeu.12410>.
- 657 [24] J.R. Hayman, S.F. Hayes, J. Amon, T.E. Nash, Developmental expression of
658 two spore wall proteins during maturation of the microsporidian
659 *Encephalitozoon intestinalis*, *Infect. Immun.* 69 (2001) 7057–7066.

- 660 <https://doi.org/10.1128/IAI.69.11.7057-7066.2001>.
- 661 [25] J.R. Hayman, T.R. Southern, T.E. Nash, Role of sulfated glycans in adherence
662 of the microsporidian *Encephalitozoon intestinalis* to host cells in vitro, *Infect.*
663 *Immun.* 73 (2005) 841–848. <https://doi.org/10.1128/IAI.73.2.841-848.2005>.
- 664 [26] Y. Li, Z. Wu, G. Pan, W. He, R. Zhang, J. Hu, Z. Zhou, Identification of a novel
665 spore wall protein (SWP26) from microsporidia *Nosema bombycis*, *Int. J.*
666 *Parasitol.* 39 (2009) 391–398. <https://doi.org/10.1016/j.ijpara.2008.08.011>.
- 667 [27] T.R. Southern, C.E. Jolly, M.E. Lester, J.R. Hayman, EnP1, a microsporidian
668 spore wall protein that enables spores to adhere to and infect host cells in vitro,
669 *Euk. Cell.* 6 (2007) 1354–1362. <https://doi.org/10.1128/EC.00113-07>.
- 670 [28] Z. Wu, Y. Li, G. Pan, Z. Zhou, Z. Xiang, SWP25, a novel protein associated
671 with the *Nosema bombycis* endospore, *J. Euk. Microbiol.* 56 (2009) 113–118.
672 <https://doi.org/10.1111/j.1550-7408.2008.00375.x>.
- 673 [29] C.A. Leonard, *Microsporidia Spore Adherence and Host Cell Infection In Vitro*,
674 East Tennessee State University, 2013.
- 675 [30] F. Zhu, Z. Shen, J. Hou, J. Zhang, T. Geng, X. Tang, L. Xu, X. Guo,
676 Identification of a protein interacting with the spore wall protein SWP26 of
677 *Nosema bombycis* in a cultured BmN cell line of silkworm, *Infect. Genet. Evol.*
678 17 (2013) 38–45. <https://doi.org/10.1016/j.meegid.2013.03.029>.
- 679 [31] B. Han, V. Polonais, T. Sugi, R. Yakubu, P.M. Takvorian, A. Cali, K. Maier, M.
680 Long, M. Levy, H.B. Tanowitz, G. Pan, F. Delbac, Z. Zhou, L.M. Weiss, The
681 role of microsporidian polar tube protein 4 (PTP4) in host cell infection, *PLoS*
682 *Pathog.* 13 (2017) 1–28. <https://doi.org/10.1371/journal.ppat.1006341>.
- 683 [32] S.E. Campbell, T.A. Williams, A. Yousuf, D.M. Soanes, K.H. Paszkiewicz,
684 B.A.P. Williams, *The Genome of Spraguea lophii and the Basis of Host-*

- 685 Microsporidian Interactions, PLoS Genet. 9 (2013) 1–15.
686 <https://doi.org/10.1371/journal.pgen.1003676>.
- 687 [33] H. Liu, M. Li, S. Cai, X. He, Y. Shao, X. Lu, Ricin-B-lectin enhances
688 microsporidia *Nosema bombycis* infection in BmN cells from silkworm *Bombyx*
689 *mori*, Acta Biochim. Biophys. Sin. 48 (2016) 1050–1057.
690 <https://doi.org/10.1093/abbs/gmw093>.
- 691 [34] R.D. Cummings, R.L. Schnaar, R-Type Lectins, in: A. Varki, R. Cummings, J.
692 Esko, H. Freeze, G. Hart, J. Marth (Eds.), Essentials Glycobiol., 3rd ed., Cold
693 Spring Harbor Laboratory Press, Cold Spring Harbor (NY), 2017.
694 <https://doi.org/10.1101/glycobiology.3e.031>.
- 695 [35] K. Sandvig, Entry of ricin and Shiga toxin into cells: molecular mechanisms and
696 medical perspectives, EMBO J. 19 (2000) 5943–5950.
697 <https://doi.org/10.1093/emboj/19.22.5943>.
- 698 [36] S. Olsnes, The history of ricin, abrin and related toxins, Toxicol. 44 (2004)
699 361–370. <https://doi.org/10.1016/j.toxicol.2004.05.003>.
- 700 [37] A. Varki, R. Cummings, J. Esko, H. Freeze, G. Hart, J. Marth, Part IV, Glucan-
701 binding Proteins, in: A. Varki, R. Cummings, J. Esko, H. Freeze, G. Hart, J.
702 Marth (Eds.), Essentials Glycobiol., 2nd ed., Cold Spring Harbor Laboratory
703 Press, 2009. <https://www.ncbi.nlm.nih.gov/books/NBK20728/>.
- 704 [38] R.V. Romero, R. Osicka, P. Sebo, Filamentous hemagglutinin of *Bordetella*
705 *pertussis*: A key adhesin with immunomodulatory properties?, Futur. Microbiol.
706 9 (2014) 1339–1360. <https://doi.org/10.2217/fmb.14.77>.
- 707 [39] S.M. Prasad, Y. Yin, E. Rodzinski, E.I. Tuomanen, H. Robert Masure,
708 Identification of a Carbohydrate Recognition Domain in Filamentous
709 Hemagglutinin from *Bordetella pertussis*, Infect. Immun. 61 (1993) 2780–2785.

- 710 <https://doi.org/10.1128/iai.61.7.2780-2785.1993>.
- 711 [40] E. Tuomanen, H. Towbin, G. Rosenfelder, D. Braun, G. Larson, S. Gunnar, C.
712 Hansson, R. Hilli, Receptor analogs and monoclonal antibodies that inhibit
713 adherence of *Bordetella Pertussis* to human ciliated respiratory epithelial cells,
714 *J. Exp. Med.* 168 (1988) 267–277. <https://doi.org/10.184/jem.168.1.267>.
- 715 [41] W.H. Tham, J. Healer, A.F. Cowman, Erythrocyte and reticulocyte binding-like
716 proteins of *Plasmodium falciparum*, *Trends Parasitol.* 28 (2012) 23–30.
717 <https://doi.org/10.1016/j.pt.2011.10.002>.
- 718 [42] J.D. Esko, N. Sharon, *Microbial Lectins: Hemagglutinins, Adhesins, and*
719 *Toxins.*, in: A. Varki, R.D. Cummings, J.D. Esko, H.H. Freeze, P. Stanley, C.R.
720 Bertozzi, G.W. Hart, M.E. Etzler (Eds.), *Essentials Glycobiol.*, 2nd Ed., Cold
721 Spring Harbor Laboratory Press, Cold Spring Harbor (NY), 2009.
- 722 [43] A.J. Thompson, L. Cao, Y. Ma, X. Wang, J.K. Diedrich, C. Kikuchi, S. Willis, C.
723 Worth, R. McBride, J.R. Yates, J.C. Paulson, Human Influenza Virus
724 Hemagglutinins Contain Conserved Oligomannose N-Linked Glycans Allowing
725 Potent Neutralization by Lectins, *Cell Host Microbe.* 27 (2020) 1–11.
726 <https://doi.org/10.1016/j.chom.2020.03.009>.
- 727 [44] G.N. Rogers, J.C. Paulson, Receptor Determinants of Human and Animal
728 Influenza Virus Isolates: Differences in Receptor Specificity of the H3
729 Hemagglutinin Based on Species of Origin, *Virology.* 127 (1983) 361–373.
730 [https://doi.org/10.1016/0042-6822\(83\)90150-2](https://doi.org/10.1016/0042-6822(83)90150-2).
- 731 [45] J. Chen, L. Geng, M. Long, T. Li, Z. Li, D. Yang, C. Ma, H. Wu, Z. Ma, C. Li, G.
732 Pan, Z. Zhou, Identification of a novel chitin-binding spore wall protein
733 (NbSWP12) with a BAR-2 domain from *Nosema bombycis* (microsporidia),
734 *Parasitology.* 140 (2013) 1394–1402.

735 <https://doi.org/10.1017/S0031182013000875>.

736 [46] Z. Wu, Y. Li, G. Pan, X. Tan, J. Hu, Z. Zhou, Z. Xiang, Proteomic analysis of
737 spore wall proteins and identification of two spore wall proteins from *Nosema*
738 *bombycis* (Microsporidia), *Proteomics*. 8 (2008) 2447–2461.
739 <https://doi.org/10.1002/pmic.200700584>.

740 [47] J. Audi, M. Belson, M. Patel, J. Schier, J. Osterloh, Ricin Poisoning, *Jama*. 294
741 (2005) 2342–2351. <https://doi.org/10.1001/jama.294.18.2342>.

742 [48] A. Sardinha-Silva, F. Mendonça-Natividade, C. Pinzan, C. Lopes, D. Costa, D.
743 Jacot, F. Fernandes, A. Zorzetto-Fernandes, N. Gay, A. Sher, D. Jankovic, D.
744 Soldati-Favre, M. Grigg, M.C. Roque-Barreira, The lectin-specific activity of
745 *Toxoplasma gondii* microneme proteins 1 and 4 binds Toll-like receptor 2 and 4
746 N-glycans to regulate innate immune priming, *PLoS Pathog*. 15 (2019) 1–24.
747 <https://doi.org/10.1371/journal.ppat.1007871>.

748 [49] P.M. Nogueira, R.R. Assis, A.C. Torrecilhas, E.M. Saraiva, N.L. Pessoa, M.A.
749 Campos, E.F. Marialva, C.M. Ríos-Velasquez, F.A. Pessoa, N.F. Secundino,
750 J.N. Rugani, E. Nieves, S.J. Turco, M.N. Melo, R.P. Soares,
751 Lipophosphoglycans from *Leishmania amazonensis* Strains Display
752 Immunomodulatory Properties via TLR4 and Do Not Affect Sand Fly Infection,
753 *PLoS Negl. Trop. Dis.* 10 (2016) 1–17.
754 <https://doi.org/10.1371/journal.pntd.0004848>.

755 [50] M.A. Favila, N.S. Geraci, A. Jayakumar, S. Hickerson, J. Mostrom, S.J. Turco,
756 S.M. Beverley, M.A. McDowell, Differential impact of LPG-and PG-deficient
757 *Leishmania major* mutants on the immune response of human dendritic cells,
758 *PLoS Negl. Trop. Dis.* 9 (2015) 1–28.
759 <https://doi.org/10.1371/journal.pntd.0004238>.

- 760 [51] K.E.M. Persson, F.J. McCallum, L. Reiling, N.A. Lister, J. Stubbs, A.F.
761 Cowman, K. Marsh, J.G. Beeson, Variation in use of erythrocyte invasion
762 pathways by *Plasmodium falciparum* mediates evasion of human inhibitory
763 antibodies, *J. Clin. Invest.* 118 (2008) 342–351.
764 <https://doi.org/10.1172/JCI32138>.
- 765 [52] W.A. Petri, R. Haque, B.J. Mann, The bittersweet interface of parasite and
766 host: Lectin-carbohydrate interactions during human invasion by the parasite
767 *Entamoeba histolytica*, *Ann.Rev. Microbio.* 56 (2002) 39–64.
768 <https://doi.org/10.1146/annurev.micro.56.012302.160959>.
- 769 [53] W.A. Petri, R.D. Smith, P.H. Schlesinger, C.F. Murphy, J.I. Ravdin, Isolation of
770 the galactose-binding lectin that mediates the in vitro adherence of *Entamoeba*
771 *histolytica*, *J. Clin. Invest.* 80 (1987) 1238–1244.
772 <https://doi.org/10.1172/JCI113198>.
- 773 [54] V.B. Carruthers, L.D. Sibley, Sequential protein secretion from three distinct
774 organelles of *Toxoplasma gondii* accompanies invasion of human fibroblasts,
775 *Eur. J. Cell Biol.* 73 (1997) 114–23.
- 776 [55] T.M.A. Blumenschein, N. Friedrich, R.A. Childs, S. Saouros, E.P. Carpenter,
777 M.A. Campanero-Rhodes, P. Simpson, W. Chai, T. Koutroukides, M.J.
778 Blackman, T. Feizi, D. Soldati-Favre, S. Matthews, Atomic resolution insight
779 into host cell recognition by *Toxoplasma gondii*, *EMBO J.* 26 (2007) 2808–
780 2820. <https://doi.org/10.1038/sj.emboj.7601704>.
- 781 [56] S. Brecht, V.B. Carruthers, D.J.P. Ferguson, O.K. Giddings, G. Wang, U. Jäkle,
782 J.M. Harper, L.D. Sibley, D. Soldati, The *Toxoplasma* Micronemal Protein MIC4
783 Is an Adhesin Composed of Six Conserved Apple Domains, *J. Biol. Chem.* 276
784 (2001) 4119–4127. <https://doi.org/10.1074/jbc.M008294200>.

- 785 [57] E. V. Lourenço, S.R. Pereira, V.M. Faça, A.A.M. Coelho-Castelo, J.R. Mineo,
786 M.C. Roque-Barreira, L.J. Greene, A. Panunto-Castelo, *Toxoplasma gondii*
787 micronemal protein MIC1 is a lactose-binding lectin, *Glycobiology*. 11 (2001)
788 541–547. <https://doi.org/10.1093/glycob/11.7.541>.
- 789 [58] J. Marchant, B. Cowper, Y. Liu, L. Lai, C. Pinzan, J.B. Marq, N. Friedrich, K.
790 Sawmynaden, L. Liew, W. Chai, R.A. Childs, S. Saouros, P. Simpson, M.C.R.
791 Barreira, T. Feizi, D. Soldati-Favre, S. Matthews, Galactose recognition by the
792 apicomplexan parasite *Toxoplasma gondii*, *J. Biol. Chem.* 287 (2012) 16720–
793 16733. <https://doi.org/10.1074/jbc.M111.325928>.
- 794 [59] Q. Huang, Evolution of Dicer and Argonaute orthologs in microsporidian
795 parasites, *Infect. Genet. Evol.* 65 (2018) 329–332.
796 <https://doi.org/10.1016/j.meegid.2018.08.011>.
- 797 [60] I.H. Kim, D.J. Kim, W.S. Gwak, S.D. Woo, Increased survival of the honey bee
798 *Apis mellifera* infected with the microsporidian *Nosema ceranae* by effective
799 gene silencing, *Arch. Insect Biochem. Physiol.* 105 (2020) 1–12.
800 <https://doi.org/10.1002/arch.21734>.
- 801 [61] M. Saleh, G. Kumar, A.A. Abdel-Baki, M.A. Dkhil, M. El-Matbouli, S. Al-
802 Quraishy, In Vitro Gene Silencing of the Fish Microsporidian *Heterosporis*
803 *saurida* by RNA Interference, *Nucleic Acid Ther.* 26 (2016) 250–256.
804 <https://doi.org/10.1089/nat.2016.0613>.
- 805

806 **Figure 1 : A) Protein sequences of EcRBLL-1, AaRBLL-1, AaRBLL-2.** The
807 putative carbohydrate binding Ricin B Lectin superfamily (IPR035992) are indicated
808 in blue. Peptide signals obtained with SignalP for *EcRBLL-1* and *AaRBLL-2* are
809 underlined; *O*-glycosylation potential sites are indicated in bold and *N*-glycosylation in
810 bold underlined. **B) Western Blot analysis. B) Anti- *EcRBLL-1* antibody.** In lane 1,
811 total *E. cuniculi* spore protein extract. A signal was obtained at 28 kDa. **C) Anti-**
812 ***AaRBLL-1* antibody and D) Anti- *AaRBLL-2* antibody.** In lane 1, total *A. algerae*
813 spore protein extract; lane 2. **C)** A signal was obtained around 25 kDa **D)** A single
814 signal was obtained around 20 kDa.

815

816 **Figure 2 : A) Localization of EcRBLL-1 in *Encephalitozoon cuniculi*.** Spores
817 were visualized using a fluorescence microscope after a first incubation with mouse
818 polyclonal antibodies against *EcRBLL-1* followed by a second immunolabelling using
819 an anti-*E. cuniculi* rabbit serum (from naturally infected rabbit). Fluorescence labeling
820 demonstrated that the anti- *EcRBLL-1* polyclonal antibodies reacted with the polar
821 tube of the spore with an unequal labelling intensity along the polar tube. The anti-*E.*
822 *cuniculi* rabbit serum reacted as expected with the spore wall as well as the polar
823 tube of mature spore. However, when both labeling were merged, the tip of the polar
824 tube only reacted with the anti- *EcRBLL-1* polyclonal antibody (white arrow). **B)**
825 **Intensity of pixels of the immuno-localization of *EcRBLL-1* in *E. cuniculi*.**
826 Spores were visualized using a confocal microscope after incubation with antibodies
827 against *EcRBLL-1*. Afterwards, a graph of the intensity of pixels from the image was
828 obtained using Fiji ImageJ software to highlight the unequal localization of *EcRBLL-1*
829 throughout the polar tube, in particular at the tip of the polar tube (white arrow). The
830 arrowhead shows the labelling of the genetic material of the spore (in the same plane

831 as the PT labeling) using DAPI, indicating that the sporoplasm was not yet
832 transferred through the polar tube.

833 **Figure 3 : Localization of AaRBLL-1 in *A. algerae*.** Spores were visualized using a
834 fluorescence microscope after a first incubation with antibodies against AaRBLL-1
835 diluted at 1:100. **A)** Brightfield allows the observation of spores and some of the polar
836 tubes (arrows). **B)** Green fluorescence signals were observed on the spore wall
837 (arrowheads) as well as on the polar tube (arrows).

838

839 **Figure 4 : Localization of AaRBLL-2 in *A. algerae*.** Purified spores were visualized
840 using a fluorescence microscope after a first incubation with primary antibodies
841 against AaRBLL-2 diluted at 1:100. **A)** Brightfield allows the observation of spores
842 and some of the polar tubes (arrows). **B)** Green fluorescence signals were observed
843 on polar tubes **C)** as well as on spore wall (arrowheads).

844

845 **Figure 5 : Antimicrosporidian activities of anti- *EcRBLL-1* antibody and**
846 **rec*EcRBLL-1*.** Inhibition assay was performed using non-cytotoxic concentrations of
847 the **A)** anti- *EcRBLL-1* antibody at 1:100 and **B)** rec*EcRBLL-1* (25 $\mu\text{g mL}^{-1}$) on *E.*
848 *cuniculi*-infected MRC-5 cells. Parasite proliferation was measured 7 days post-
849 infection. **A)** and **B)** each represent only one independent experiment from two **A)**
850 and five **B)** replicates. Each condition was done in triplicate. Parasite proliferation
851 was analyzed by comparing treated conditions to the infected untreated control using
852 a Wilcox test. Differences were considered significant if the *p* value was < 0.001 (*).
853 **A)** A decrease on average of 12.3% in the growth of the parasite was observed when
854 cells were infected with 2×10^5 spores pre-treated with anti-*EcRBLL-1*. **B)** A pre-
855 treatment of MRC-5 cells was done with 25 $\mu\text{g mL}^{-1}$ of rec*EcRBLL-1* followed by an

856 infection with 2×10^5 spores. A reduction on average of 23.7% of parasite growth
857 was observed.

858

859 **Figure 6 : Antimicrosporidian activities of recAaRBLL-2 and anti-AaRBLL-2,**
860 **anti-AaRBLL-1 polyclonal antibodies.** Inhibition assay was done by pre-treating a
861 solution of *A. algerae* spores with each polyclonal antibody at 1:100. After a quick
862 PBS wash, spores were put in contact with HFF cells for 5 days. Parasite proliferation
863 was then visualized by a FISH method. Results originate from 3 independent
864 infection repeated twice. The percentage of infected cells was assessed by counting
865 cell nuclei and infectious foci in 10 randomly chosen fields on three coverslips.
866 Parasite proliferation was analyzed by comparing treated conditions to the infected
867 untreated control using a Wilcox test. Differences were considered significant if the *p*
868 value was < 0.001 (**). The control group are non-treated infected cells. Compared to
869 the control group, pre-treatments with *recAaRBLL-2*, anti-AaRBLL-2 and anti-
870 AaRBLL-1 decreased the parasite proliferation on average by 59.3%, 68.5% and
871 67.6% respectively.

872

873

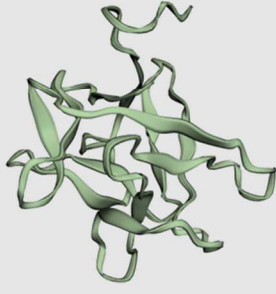
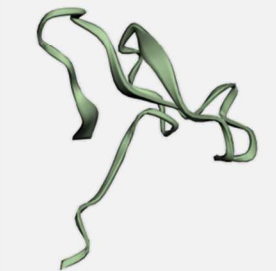
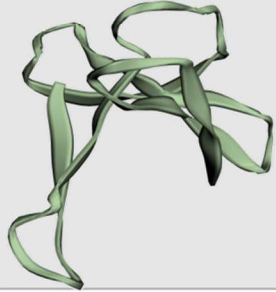
874

875

876

877

Table 1 : Structure and functional analysis of the RBLL proteins obtained with Phyre2 online software.

Proteins	3D model	Secondary structure	Superfamily / family /PDB molecule	Confidence	% identity
<i>EcRBLL-1</i> (ECU08_1730)		α helix (8%) β strand (41%)	β -glucanase	98.8	20
			Ricin-B-like lectin	98.6	17
			Sugar binding protein	98.4	16
			Hemagglutinin component	98.2	13
<i>AaRBLL-1</i> (MZ547653)		α helix (18%) β strand (47%)	Ricin-B-like lectin	96.1	32
			Agglutinin-1 b chain	95.5	20
			Hemagglutinin component	95.3	23
			β -glucanase	93.5	38
<i>AaRBLL-2</i> (MZ547654)		α helix (2%) β strand (50%)	β -glucanase	91.5	21
			Ricin-B-like lectin	91.4	24
			Hemagglutinin component	85.2	23
			Agglutinin	81.4	20

According to this algorithm, the likely accuracy of the model is determined by the percentage identity between our sequences and templates. Moreover, a low sequence identity (<15%) model can be useful as long as the confidence is high. A match with a confidence >90%, indicates that the protein adopts the overall fold shown in the 3D model.

A

EcRBL-1 (ECU08_1730)

MMLIALCMMGVVLGFKITAKNNEGKFLINNGKAVMSESGKPAEFKTDEVSPGVKIVTDK
NTNKVLDIEGSKTNLIFYSRHGQENQRFTFVGGEGDVIIYIKSGDGCLEYDSNGKMYRTTC
SAKDQQRFKIVYSLGDPGYKPPVEVPVPAAPEN**NPST**QDLLE**SPSS**QALSGSANAHAPPQV
LIFNGKKSHR**SHS**WHHNPYEDESSIYGSDCLIV

AaRBL-1 (MZ547653)

MLIFFLSIKTLLIKVQNNLGFVAFDGTLYLFQTPNIKE**ASEFEFIQN**ENGIDFYIQLAKTN
LVWDYPRQDFGGNIILYRFHGGSNQKWRLIFNKLGSNLNIVNNDRRVVYNEYTNLFTTKKI
NEYMNGEEGFVIFDEKMHYFDFFNHVPVQNIIMNVPSIEHLLPLGKELRKPS**PNIGGPSSA**
PPIMPLGPNMHEQMFLNQMG

AaRBL-2 (MZ547654)

MTLTKYIIILSLFINYSISFVIQERSTGRYLSSKNMGVVALVEDIRQASPYIIRAVGNP
IDMAITDKKSKLALDFAADGPDLSYSYSSSTNQLFKLNLDENGYWQIIQGTEKYLYYDP
ETSKLKGOPYDVSKTVGFMLFADDGIGPFVPMKGAKLP**SPI**PPVYPEAPLLPENEASFAP
K*

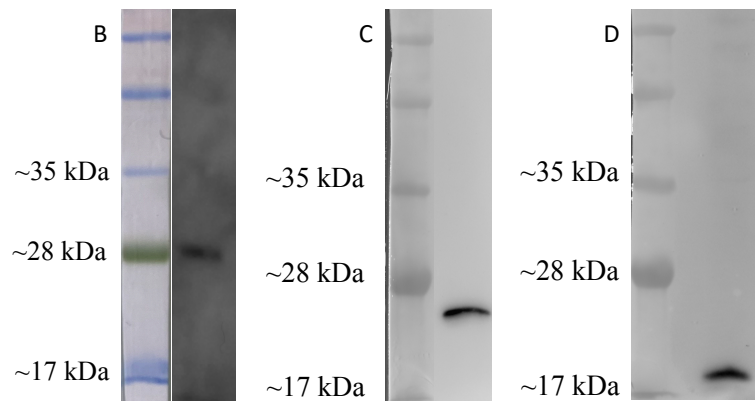


Fig. 1

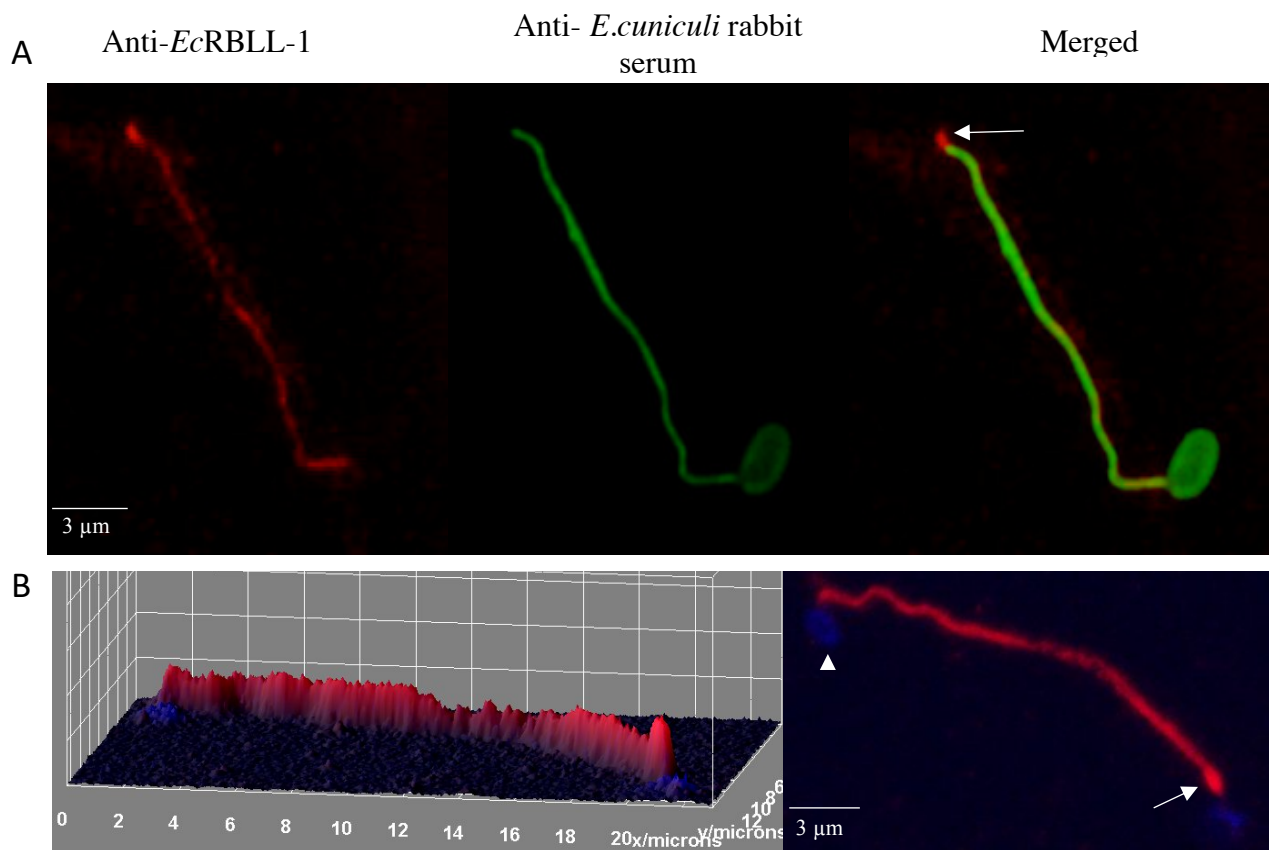


Fig. 2

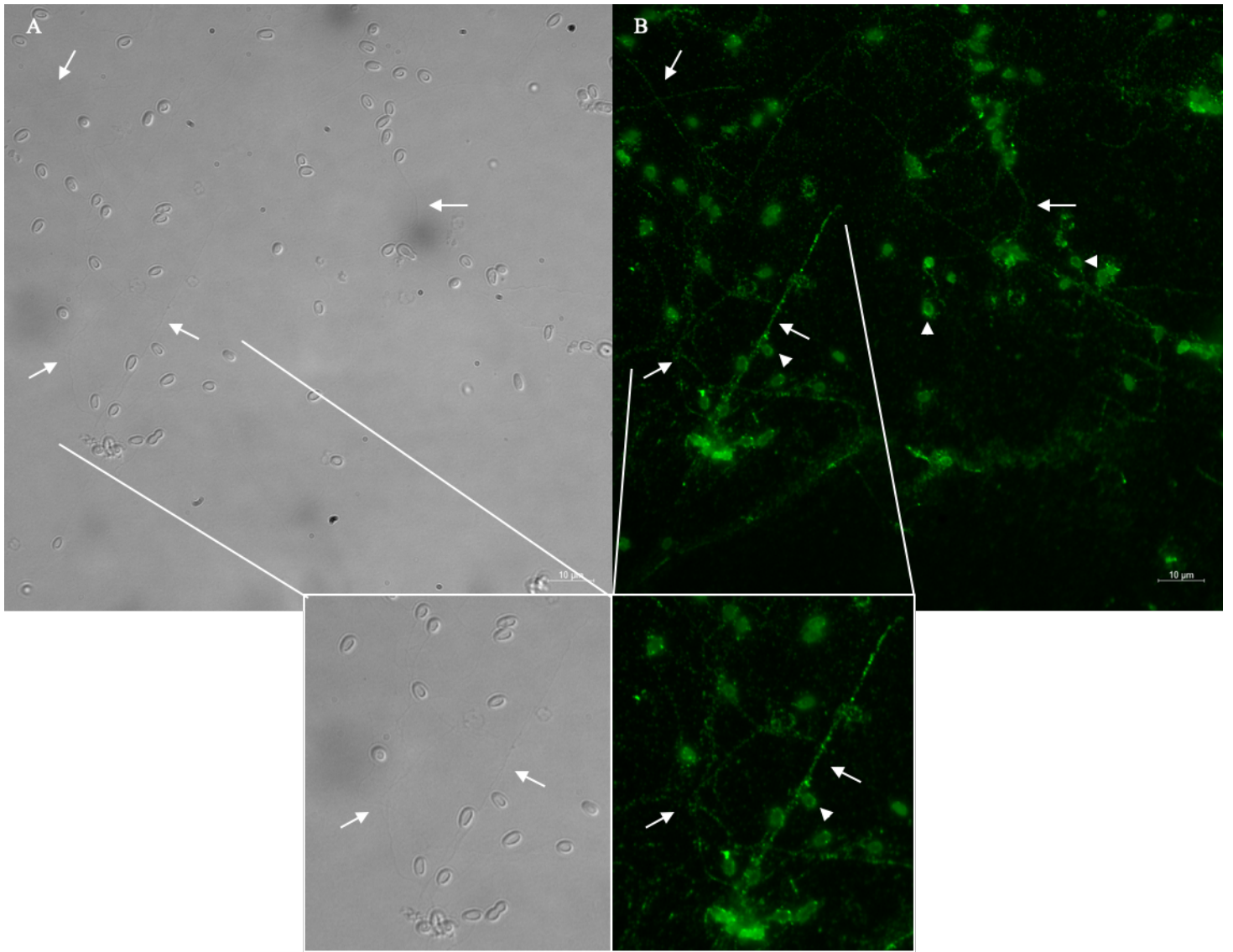


Fig. 3

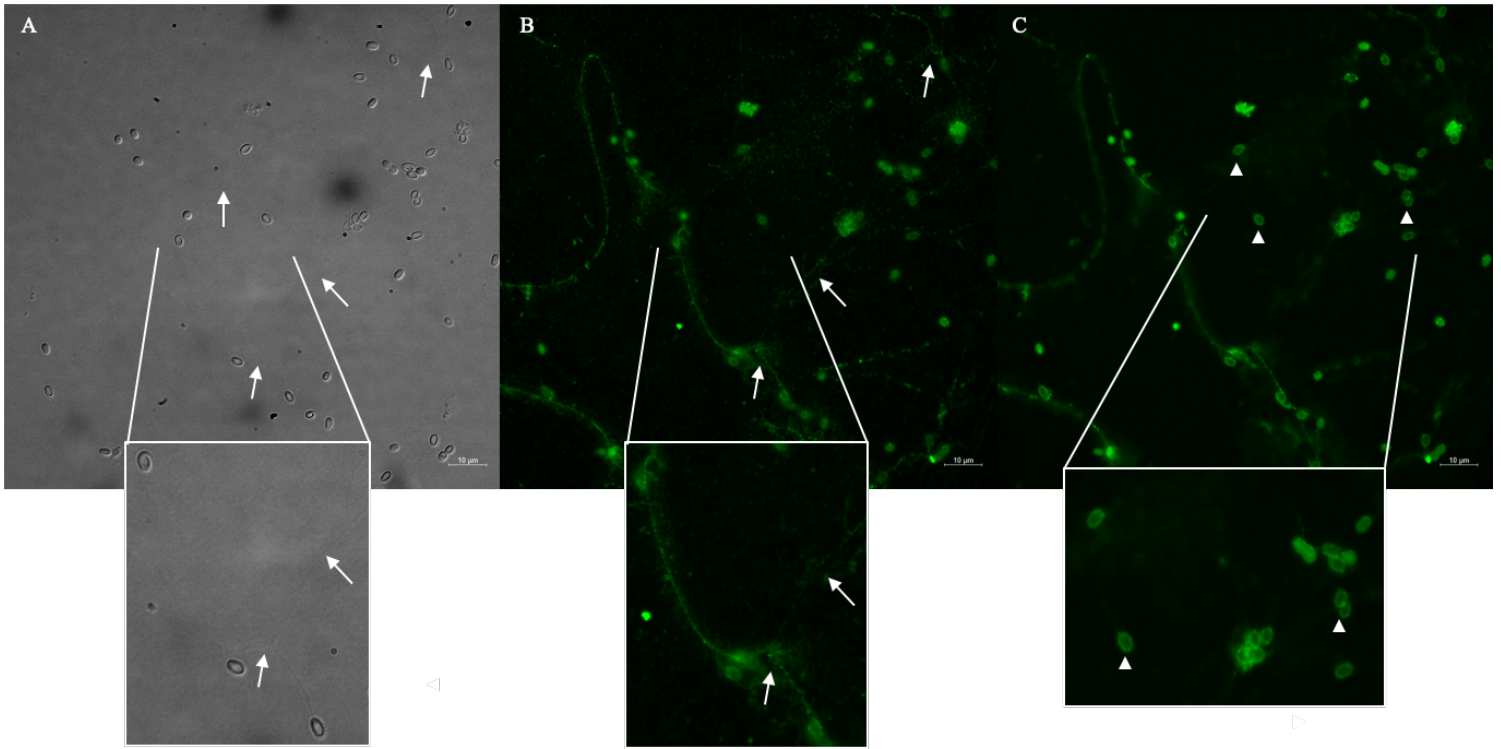


Fig. 4

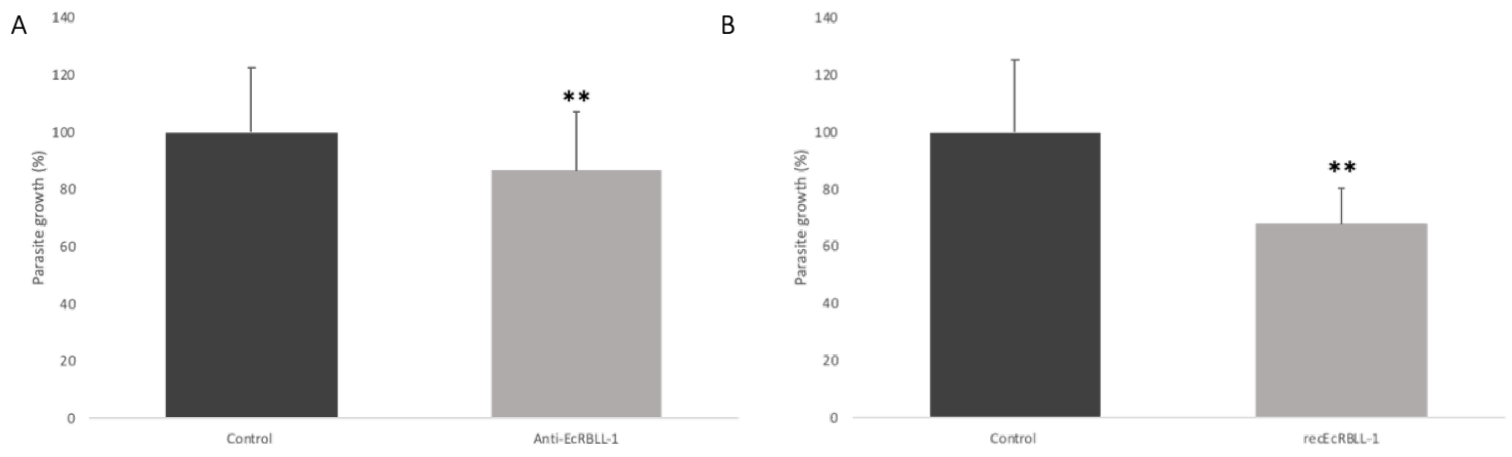


Fig. 5

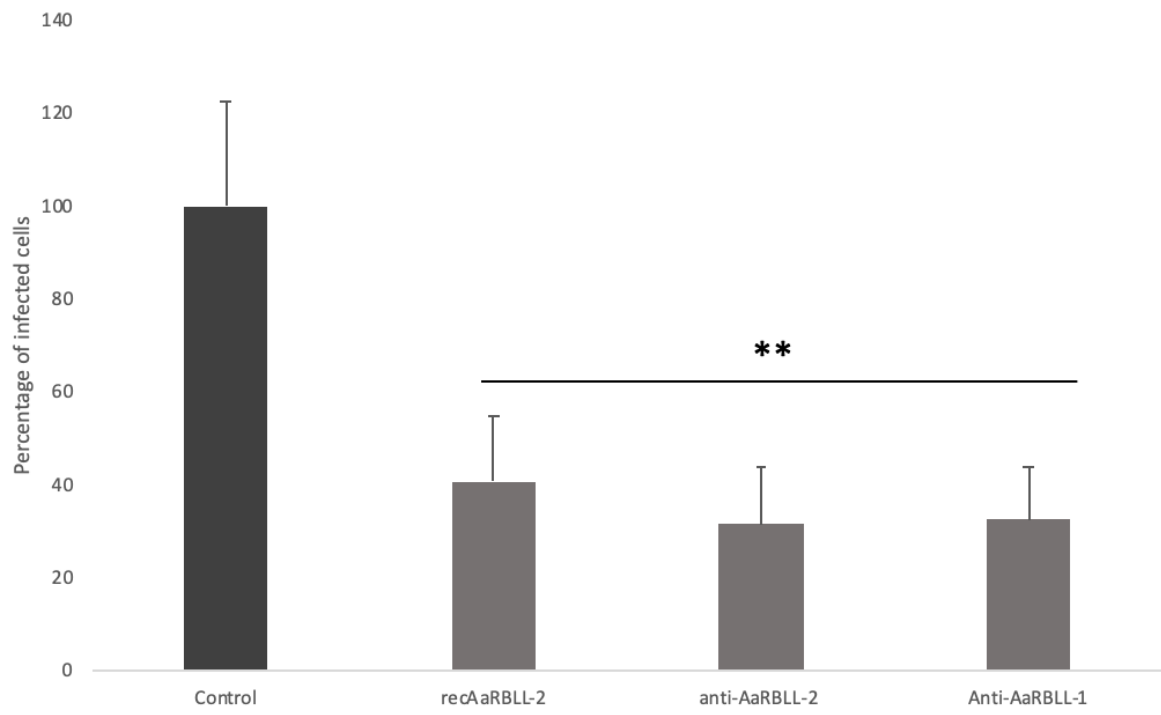
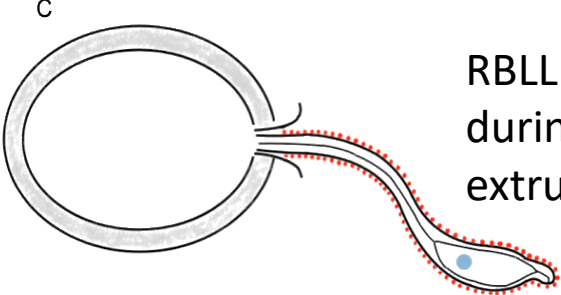
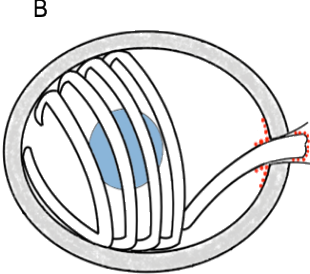
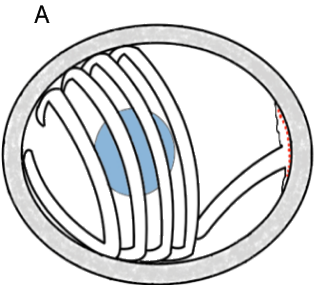


Fig.6

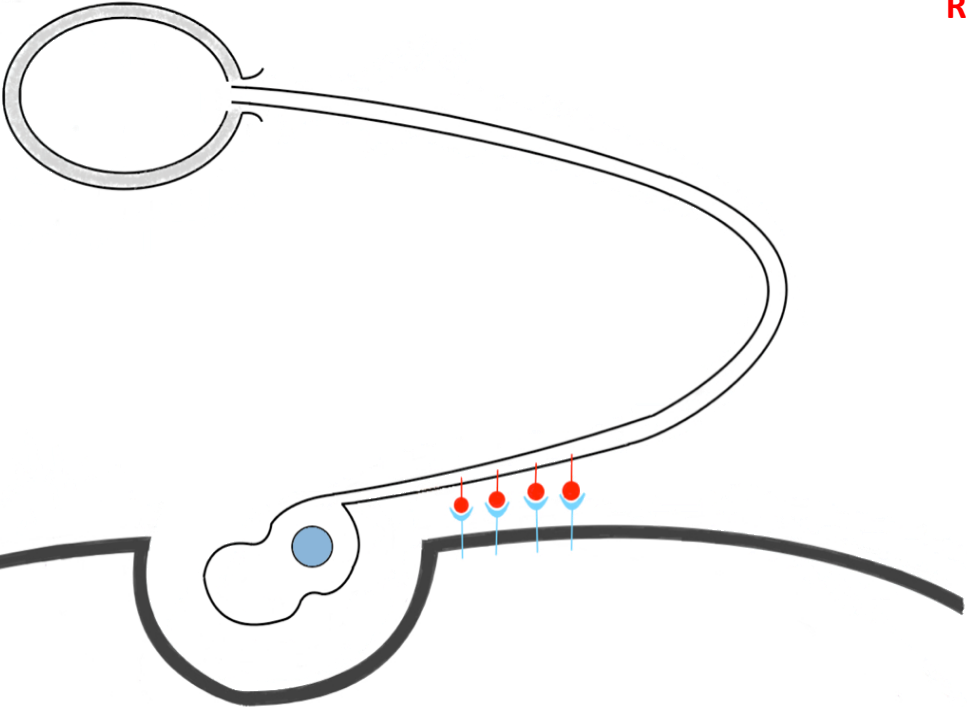
Microsporidian spore



RBLL release during polar tube extrusion

RBLL Proteins

D



RBLL Proteins

Host cell receptors